Climate Dynamics (1998) 14:451–460

L.-B. Tremblay · L. A. Mysak

On the origin and evolution of sea-ice anomalies in the Beaufort-Chukchi Sea

Received: 1 May 1997/Accepted: 22 October 1997

Abstract The origin and space-time evolution of Beaufort-Chukchi Sea ice anomalies are studied using data and a recently developed dynamic-thermodynamic sea-ice model. First, the relative importance of anomalies of river runoff, atmospheric temperature and wind in creating anomalous sea-ice conditions in the Beaufort-Chukchi Sea is investigated. The results indicate that wind anomalies are the dominant factor responsible for creating interannual variability in the Beaufort-Chukchi Sea ice cover. Temperature anomalies appear to play a major role for longer time scale fluctuations, whereas the effects of runoff anomalies are small. The sea-ice model is then used to track the position of a positive sea-ice anomaly as it is transported by the Beaufort Gyre toward the Transpolar Drift Stream and then exported out of the Arctic Basin into the Greenland Sea via Fram Strait. The model integration shows that sea-ice anomalies originating in the western Beaufort Sea can survive a few seasonal cycles as they propogate through the Arctic Basin and can account for a notable amount of anomalous ice export into the Greenland Sea. These anomalies, however, represent a small contribution to the fresh water budget in this area when compared with sea-ice fluctuations generated by interannually varying local winds.

1 Introduction

Large interannual and decadal time scale variations occur in the Arctic sea-ice areal extent, especially in summer, when large parts of the peripheral seas are relatively free of ice. These variations result in a different positioning of the ice margin on these time scales. In this study, certain aspects of these ice cover anomalies are described and modelled, with the emphasis on the interannual time scale fluctuations. [By anomalies we mean the difference between the sea-ice cover for a given month in a particular year and the climatological value for that month.]

In a study of interdecadal climate variability in the Arctic, it has been hypothesized (Mysak et al. 1990) that ice anomalies originating in the Beaufort-Chukchi Sea region travel out of the Arctic into the Greenland Sea via the Beaufort Gyre and the Transpolar Drift Stream. This hypothesis was further explored in Mysak and and Power (1992) who showed from a cross-correlation analysis that Beaufort Sea ice concentration anomalies propagated into the Greenland Sea in about two to three years. This process would contribute to variations in the transport of sea ice (and hence fresh water) into the Greenland Sea and could potentially affect the local ocean circulation there (Aagaard and Carmack 1989). Since deep convection occurs in the Greenland Sea, the input of substantial amounts of fresh water from the Arctic could possibly stabilize the water column and suppress or reduce convection in that region. This in turn could reduce deep water formation in the northern North Atlantic and consequently decrease the poleward heat transport via the thermohaline circulation (Broecker et al. 1985). Hence, sea-ice conditions in the peripheral seas and variations in sea-ice export from the Arctic are important factors to consider in climate studies of high-latitude regions.

The anomalous ice export into the Greenland Sea during the 1960s associated with the "Great Salinity Anomaly" was originally explained by the forcing from local wind anomalies (Dickson et al. 1975). More recently, the importance of large-scale wind anomalies over the central Arctic in generating ice anomalies was recognized (Walsh and Chapman 1990). Simulation

L.-B. Tremblay[1] (✉) and L.A. Mysak
Department of Atmospheric and Oceanic Sciences and Centre for Climate and Global Change Research, McGill University, 805 Sherbrooke St. West, Montreal, Quebec H3A 2K6, Canada

Present address:
[1]Lamont-Doherty Earth Observatory of Columbia University, Palisades, New York

results from a coupled sea ice-ocean model (Häkkinen 1993) show that a large part of the fluctuations in ice export out of the Arctic can be explained by regional and large-scale anomalous wind patterns, which supports the latter hypothesis. Other sources of fluctuations in the fresh water budget for the Greenland Sea include the variation of surface Arctic Ocean salinity caused by fluctuations in the river runoff into the Arctic (Mysak et al. 1990) and the input of relatively fresher water through Bering Strait (Goose et al. 1997).

A number of studies have set out to identify the main factors responsible for the occurrence of ice anomalies in the Beaufort-Chukchi Sea. From a cross-correlation analysis, Manak and Mysak (1989) found that ice anomalies in the Beaufort-Chukchi Sea could be linked to prior fluctuations of fresh water input from Mackenzie River runoff. Such runoff, it was argued, would raise the freezing point temperature of ocean water and thus increase ice growth during the cold season. Recent simulation results from a coupled sea ice-ocean model (Weatherly and Walsh 1996), however, showed that the doubling of Arctic river runoff has little effect on sea-ice formation. These results are open to debate, though, because of the relatively coarse resolution in the model which does not allow an accurate representation of river runoff-sea ice interactions.

Rogers (1977), on the other hand, found that interannual ice anomalies in the Beaufort Sea were correlated with anomalous atmospheric temperature and wind patterns, with wind forcing being the dominant factor. Chouinard et al. (1995) studied the relation between Beaufort Sea ice anomalies and sea surface temperature, anomalous wind patterns and discharge from the Mackenzie River using empirical orthogonal function (EOF) analysis. The data used come from Beaufort Sea weekly ice charts produced by the Atmospheric Environment Service of Canada. The first sea-ice EOF (explaining 45% of the total variance) showed a north-south displacement of the ice edge, which was interpreted to be due to anomalous air temperature conditions. The second EOF (explaining 35% of the total variance) showed an east-west structure of the data, which was believed to be due to anomalous ice conditions produced by winds. A recent re-analysis (Chouinard and Guarrigues personal communication) revealed that the third and fourth EOFs show an ice anomaly shaped like a river plume at the mouth of the Mackenzie delta, and that together, they account for less than 10% of the total variance. These two EOFs are believed to be associated with river runoff.

In this work, we use oceanic, sea-ice concentration and atmospheric data, and a recently developed sea-ice model (Tremblay and Mysak 1997) to determine the relative importance of anomalous ocean surface salinities, atmospheric temperatures and winds, in creating ice anomalies in the Beaufort-Chukchi Sea region. Since the model does not include a fresh water budget, the possible influence of river runoff on ice anomalies will be estimated from simple budget calculations and relevant observations. The influence of temperature and wind anomalies, however, is assessed from large-scale temperature and wind stress data together with a model simulation of the Arctic sea-ice cover for the year 1965, when one of the largest positive ice anomalies was observed in the Beaufort-Chukchi Sea. The sea-ice model is also used to track a large western Beaufort Sea ice anomaly around the Beaufort Gyre and determine whether it can survive a few seasonal cycles and still cause a notable fluctuation of ice export into the Greenland Sea via Fram Strait.

Section 2 very briefly describes the ice model used in the simulation of the Arctic sea-ice cover. Section 3 discusses the various mechanisms that could lead to the formation of ice anomalies in the Beaufort-Chukchi Sea. In Sect. 4, the space-time evolution of a large ice anomaly initially placed in the western Beaufort Sea is modelled. The main conclusions drawn from this study are summarized in Sect. 5.

2 Sea-ice model

For large-scale simulation of the Arctic sea-ice cover forced by monthly averaged wind stress, both the advection and acceleration terms can be neglected in the two-dimensional sea-ice momentum equation. The remaining terms in the momentum equation include the wind shear stress on the top of the ice, the ocean drag, the internal ice stress term resulting from ice flow interactions, the sea surface tilt term and the Coriolis term. The wind stress and ocean drag are obtained from a simple quadratic law with constant turning angle (McPhee 1975).

In this model, the sea-ice is assumed to behave as a granular material in slow continuous deformation. The resistance of sea-ice to compressive load is considered to be a function of its thickness and concentration, and its shear resistance is proportional to the internal ice pressure at a point. In divergent motion, the ice offers no resistance, and the floes drift freely. A detailed description of the sea-ice dynamic and thermodynamic models can be found in Tremblay and Mysak (1997).

3 Origin of ice anomalies in the Beaufort-Chukchi Sea

During a given year, the surface area covered by sea-ice in the Beaufort-Chukchi Sea can differ substantially from climatology. In this region, one of the largest summer ice anomalies, inferred from satellite and other measurements made over the second half of this century, occurred during 1964–67. This positive ice anomaly signal in the combined Beaufort-Chukchi Sea region peaked at 150×10^3 km^2 (Fig. 1), which was approximately 25% of the total climatological uncovered area in this region. If this anomaly was of the order of 1 m thick in this region, then this corresponds to an ice volume anomaly of 150 km^3 (the mean ice thickness in this region is 2–3 m (Bourke and Garrett 1987)).

Sea-ice thickness can vary because of both thermodynamic and dynamic processes, as indicated by the

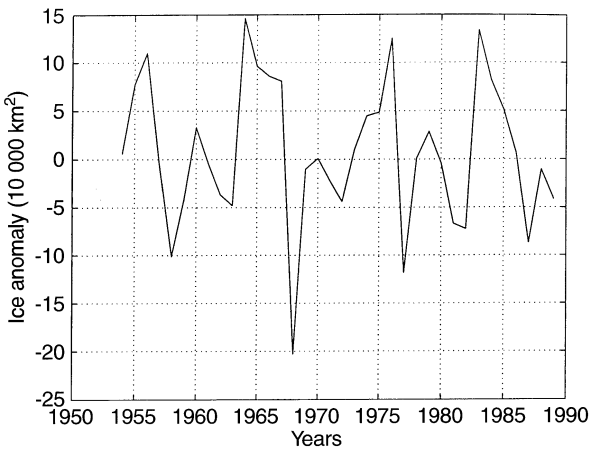

Fig. 1 Summer sea-ice anomaly time series for the Beaufort and Chukchi seas as defined by region 2 in Mysak and Manak (1989) (data from Walsh and Chapman 1995, personal communication)

sea-ice countinuity Eq. (1). To understand better the influence of these two factors on the growth of sea-ice, the time scale associated with each of these processes is determined. The sea-ice continuity equation can be written as follows:

$$\frac{\partial h}{\partial t} + \nabla \cdot (\boldsymbol{u}_i h) = S_h, \tag{1}$$

where h is the mean ice thickness, $\boldsymbol{u}_i$ the ice velocity and S_h the thermodynamic source term.

To estimate the time scale involved in the growth of sea-ice due to thermodynamic processes, we assume the first term in Eq. (1) is in balance with the forcing term. This yields

$$[t]_{temp} = \frac{[h]}{[S_h]} = \frac{3\text{ m}}{0.3\text{ cm/day}} \approx \text{three years},$$

assuming a mean ice thickness of 3 m and a typical ice growth of 0.3 cm/day (Maykut and Untersteiner 1971). Similarly, the time scale of sea-ice growth due to dynamical processes can be found by balancing the second term with the first term. This gives

$$[t]_{wind} = \frac{[L]}{[U]} = \frac{300\text{ km}}{5\text{ cm/s}} \approx \text{two months},$$

where $[L]$ is the Beaufort-Chukchi Sea half width (300 km) and $[U]$ is a typical ice drift speed (5 cm/s). From the above estimates we conclude that dynamic effects will contribute more rapidly to interannual variability of the sea-ice cover than thermodynamic effects.

The time scale for salinity change associated with river runoff is more difficult to estimate since it has an effect on both ocean stratification and ocean surface salinity. This is discussed in detail in the next section.

3.1 Salinity hypothesis

To obtain an estimate of the effect of reduced sea surface salinity (due to enhanced Mackenzie River runoff) on ice formation during the fall in the ice-free region of the Beaufort Sea, two idealized initial states are considered: first, a reference two-layer ocean [In the Beaufort Sea (away from the month of the Mackenzie river), the vertical structure of the ocean is more complex with the presence of surface Artic, North Pacific (entering through Bering Strait), intermediate and deep waters (Agaard *et al.* 1985); this is ignored in the following simple analysis.] with climatological sea surface salinity ($\bar{S}$), and second, a perturbed two-layer ocean with reduced sea surface salinity (S') due to increased river runoff. The initial temperature of the ocean mixed-layer in the fall is considered to be $T_0 = 0\,^\circ$C. A reduction of sea surface salinity results not only in a higher freezing point temperature (Manak and Mysak 1989), but also in a stronger upper ocean stratification. These two factors contribute to an enhanced ice formation in the fall. In the following, we present a first order calculation to quantify the combined effect of these two factors.

In the reference (climatological) case, the total heat released by the mixed layer to reach its freezing point temperature in the fall is equal to $\rho_w A_{BS} H_{ml} C_{pw}[T_0 - T_{fp}(\bar{S})]$, where ρ_w is the density of water, A_{BS} the Beaufort Sea ice-free surface area (300×10^3 km^2), H_{ml} the reference case mixed-layer depth (assume equal to 20 m), C_{pw} the specific heat of water (4×10^3 J/K) and $T_{fp}(\bar{S})$ the freezing point of water with salinity $\bar{S}$ ($-1.8\,^\circ$C for $\bar{S} = 31$ ppt). To provide an **upper bound** on the ice anomaly estimate, we assume the fresher ocean loses the same amount of heat to the atmosphere at that time and in the process also forms a thin ice layer. Thus the heat loss is made up of two components, the heat required to cool the ocean mixed layer from $0\,^\circ$C to its freezing point temperature, and the latent heat released during anomalous ice formation. The thickness of the ice anomaly h_{ia} can be calculated as follows:

$$\rho_w A_{BS} H_{ml} C_{pw}[T_0 - T_{fp}(\bar{S})] = \rho_w A_{BS} h_{ml} C_{pw}[T_0 - T_{fp}(S')] + \rho_i A_{BS} L_f h_{ia},$$

which yields

$$h_{ia} = \frac{\rho_w C_{pw}}{\rho_i L_f}\{H_{ml}[T_0 - T_{fp}(\bar{S})] - h_{ml}[T_0 - T_{fp}(S')]\}, \tag{2}$$

where h_{ml} is the fresher ocean mixed-layer depth, ρ_i the density of ice and L_f the latent heat of fusion of water (3.34×10^5 J/kg K). It remains to estimate the modified mixed-layer depth (h_{ml}) and sea surface salinity (S') resulting from an abnormally high river runoff. Both of these will strongly depend on the amount of horizontal

and vertical mixing taking place during the summer months.

The amount of horizontal mixing is assessed from the ocean surface salinity for the months of May and September (from Levitus data 1994, not shown here). In the spring, the high river runoff produces a tongue of fresh water extending from the Mackenzie River mouth to the edge of the Beaufort Sea; in the fall, this fresh water signal is advected westward and much mixing occurs, resulting in surface salinities varying between 25 to 30 ppt. Accordingly, we assume that both river runoff and melted sea-ice are well mixed horizontally in the ocean surface layer. On average, the annual river runoff ($300\,km^3$) and melting of first year ice ($300 \times 10^3\ km^2 \times 1$ m) contribute equally to the input of fresh water into the Beaufort Sea. It is assumed that mixing of this fresh water with the saltier ocean water due to the winds, tides and waves produces a 20 m deep mixed layer (H_{ml}) and a 3.1 ppt salinity difference between the surface and the deep water (see Fig. 5 in Appendix A). Assuming the same amount of energy input into the fresher ocean mixed layer due to mixing, a $50\,km^3$ river runoff anomaly (8% anomaly of the total fresh water input), as observed in the 1965 (Mysak and Power 1992), will produce a 1.2 m reduction in mixed-layer depth (Eq. 4 in Appendix A) and a 0.48 ppt reduction in mixed layer salinity (Eq. 3 in Appendix A). Detailed calculations for these numbers are presented in Appendix A. Considering a linear dependence of the ocean freezing point temperature on salinity, this reduction in sea surface salinity results in a $0.028\,^{\circ}C$ increase in freezing point temperature ($T_{fp}(S')$) relative to the reference case ($T_{fp}(\bar{S})$).

Upon substituting these values into Eq. 2, we obtain an upper bound on the ice anomaly estimate (h_{ia}) of 3.7 cm. An ice layer of this thickness will lead to a slightly thicker winter ice cover and could prevent complete melting the following summer. [The maximum correlation between river runoff and sea-ice extent is found at a lag of one year (Manak and Mysak, 1989; Chouinard and Garrigues 1995).] However, a 3.7 cm ice thickness anomaly only constitutes a 4% increase over the Beaufort Sea first year ice thickness (1 m) in winter and is considered of minor importance in explaining interannual variability in this region. This agrees with the conclusion drawn from an EOF analysis of Beaufort Sea ice data (Chouinard and Garrigues, personal communication), where the third and fourth modes (believed to be related to the discharge of the Mackenzie River), explains less than 10% of the total variance. Also, the influence of **reduced fresh water input** into the Arctic seems to be more important than an increased input (see Appendix A). Its influence on the freezing point temperature of the ocean water is negligible compared with its influence on the stratification of the upper ocean, a necessary condition to have significant ice formation in the deep ocean (Aagaard and Carmack 1989). The fluctuations in the input of fresh water over longer time scales (decadal timescale), when considering all river runoff and the entire Arctic mixed-layer volume, however, could have a substantial influence on the Arctic stratification and consequently on the average thickness of the ice cover.

3.2 Atmospheric temperature and wind stress hypotheses

The possible influence of atmospheric temperature and wind stress anomalies on the formation of sea-ice anomalies in the Beaufort-Chukchi Sea is now examined. In principle, colder years result in thicker ice which prevents complete melting in the next summer, while anomalous wind patterns can advect ice southward or northward, resulting in a very different ice edge position the next summer. The anomalous years used in this study are chosen from the ice concentration anomaly time series shown in Fig. 1. An approximately 10-y oscillation is seen as the dominant signal in this figure (which confirms what was found by Mysak and Power 1992) although secondary peaks are seen in between the higher peaks. These major peaks also correlate with the peaks in the Mackenzie river runoff, as shown in Bjornsson et al. (1995).

To quantify the relative importance of atmospheric temperature and wind stress anomalies in creating ice anomalies, the sea-ice model is run from October 1964 to September 1965 (see Fig. 1) and the ice anomaly field at the end of the integration is calculated. The initial conditions used for this run are the ice drift speed, thickness and concentration for the September climatology. The model is run for one year in the uncoupled mode, first with the climatological (1959–89) monthly mean atmospheric temperature field and the anomalous (1965) monthly mean wind stress prescribed, and then with the anomalous (1965) monthly mean temperature field and the climatological monthly mean wind stress pattern. In this manner, that path of the ice anomaly explained by the temperature anomaly can be differentiated from that part explained by the anomalous wind-driven transport of ice in the Beaufort Sea. The air temperatures were calculated from the NMC 850 mb height and temperature fields, assuming a linear temperature profile from the 1013 mb and 850 mb levels whereas the wind stresses were calculated from the NMC daily sea level pressure analysis. In both cases, the temperature/wind stress at a given day is calculated as a weighted average of the mid-month climatological values.

Figure 2 shows the observed summer sea-ice edge position from the data compiled by John Walsh (University of Illinois) for climatology, Fig. 2a, and for the year 1965, Fig. 2c. In this figure, the dividing line (ice edge) between ice and no-ice was set at 75% ice concentration in order to increase the contrast between the anomalous year and climatology. In Fig. 2 the

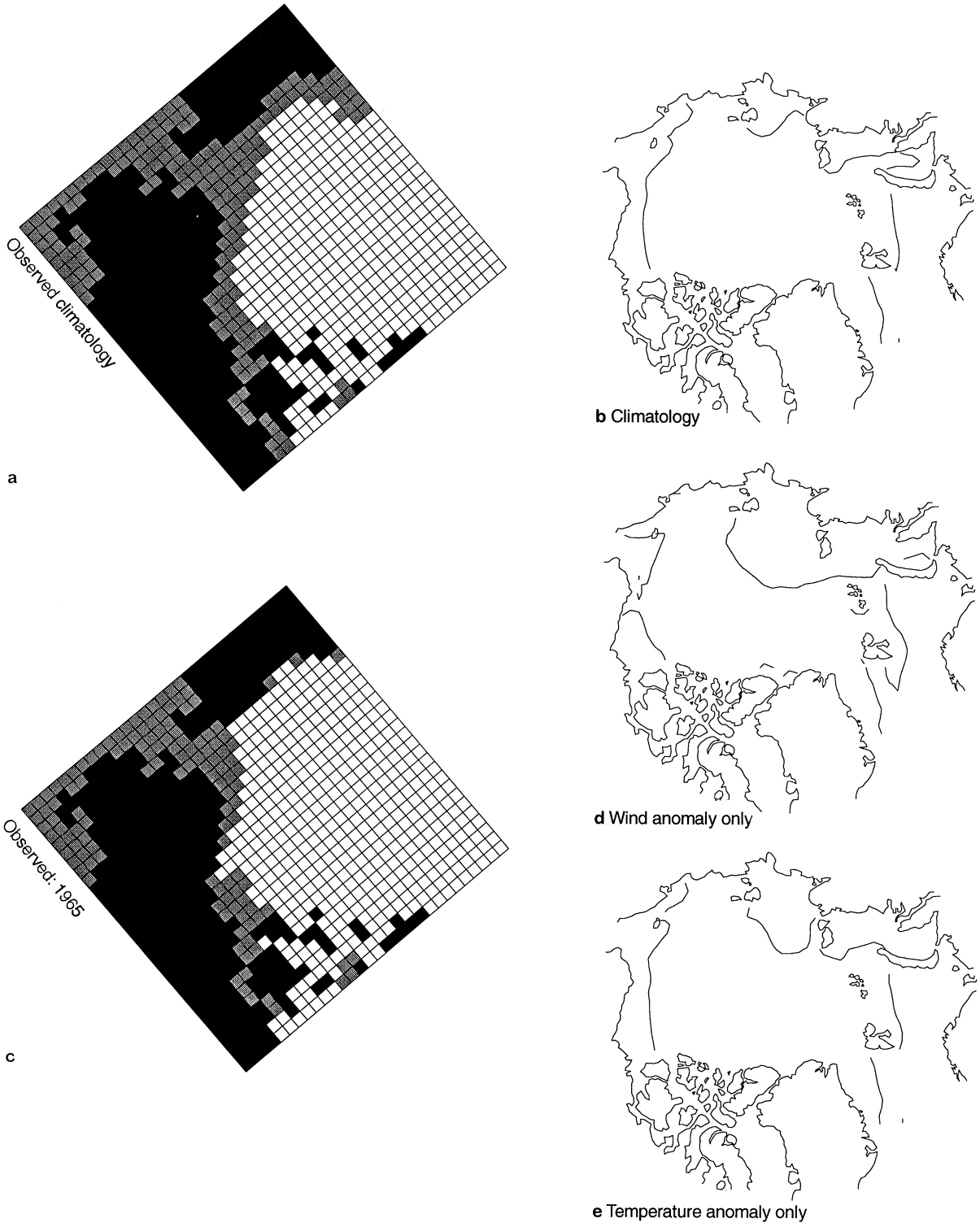

Fig. 2a–e a, c Observed and **b, d, e** simulated ice-edge position for **a, b** climatology and **c, d, e** the year 1965. In **d**, the model is forced with 1965 wind stress and climatological atmospheric temperature and in **e** the model is forced with climatological wind stress and 1965 atmospheric temperature. To increase the contrast between climatology and the anomalous year, the ice-edge position is defined as 75% ice concentration

simulated summer ice margin using climatological wind stresses and air temperatures (Fig. 2b), 1965 wind stresses and climatological air temperatures (Fig. 2d), and climatological wind stresses and 1965 air temperatures (Fig. 2e), are presented. The results for the climatology (Fig. 2b) show that the simulated ice edge position in the Beaufort-Chukchi Seas is in excellent agreement with the observations. This gives us confidence in the model's ability to reproduced observed sea-ice conditions for a particular year. In Fig. 2d, where the model is forced with prescribed climatological monthly mean temperature and 1965 wind stresses, the observed ice margin (1965) is well reproduced by the model, with anomalous ice conditions simulated in both the western Beaufort and Chukchi seas. The ice concentration and thickness anomaly in the two regions are similar and approximately equal to 20% and 2 m respectively. On the other hand, the results using prescribed climatological monthly mean wind stresses and the 1965 temperature field (Fig. 2e) resembles the climatology run in Fig. 2b; this indicates that anomalous winds are mainly responsible for the formation of the 1965 anomalous ice conditions and that the atmospheric temperature anomalies only played a minor role. The results using both 1965 wind stresses and air temperatures (not shown here) are very similar to the one in Fig. 2d.

To determine whether these conclusions are also applicable to other years where anomalous Beaufort-Chukchi Sea ice conditions were present, the monthly mean wind stress anomaly fields for eight events of abnormally high/low ice concentrations are presented and discussed in Appendix B (1956-high, 1958-low, 1965-high, 1968-low, 1976-high, 1977-low, 1983-high and 1987-low).

4 Evolution of Beaufort Sea ice anomalies

In the previous section, it is argued that the ice concentration anomalies observed in the coastal regions of the Beaufort-Chukchi Sea in 1965 are mainly due to anomalous winds advecting ice into that region. Since the ice advected towards the coast would also include multi-year ice, the anomaly near the coast will show up in both sea-ice concentration and thickness data. Here we model the time evolution of the western Beaufort Sea ice anomaly observed in 1965 as it is advected around the Beaufort Gyre. At first, the model is run for a period of 3 y starting in October 1965 with an ice anomaly of 2 m in mean thickness and of 20% in ice concentration as the initial conditions (see second last paragraph of Sect. 3.2 and Fig. 3a, and also 2c), and with 1965-66-67 wind stress and atmospheric temperature forcing fields. In a second calculation, the model is run with the same forcing but with the September climatological ice thickness and concentration field as the initial conditions. The anomaly signal for a given time, is constructed by subtracting the output of the run with climatological initial conditions from the output of the run with anomalous ice conditions.

Figure 3 shows the difference ice thickness fields between the two runs (as described) at time intervals of six months. The ice anomaly is advected anti-cyclonically around the Beaufort Gyre and into Fram Strait, and is clearly apparent over 2 y later (spring 1968) in the Greenland Sea region. Similar conclusions were drawn by Chapman et al. (1994) who traced ice thickness anomalies around the Beaufort Gyre and Transpolar Drift Stream and by Mysak and Power (1992) who traced ice concentration anomalies along the same transect. In the peripheral seas, the ice anomaly signal decreases in amplitude as it is in contact with warmer waters from the ice free area; in the central Arctic, summer melting is more important than winter ice growth for thicker ice, which leads to a further reduction in the amplitude of the signal. From the Beaufort Sea to the Fram Strait, the ice anomaly has decreased from 2 m to approximately 20 cm (Fig. 3e). Considering a mean spring ice thickness of 3 m (Bourke and Garrett 1987) in the Fram Strait region, this can account for a 7% ice volume anomaly. In 1968, an ice concentration anomaly of 300 000 km^2, attributed to local and large-scale wind anomalies in the high Arctic, constituted at least 25% increase in the ice export over the climatological value. In fact, the ice exported that year was probably thicker as the large-scale wind pattern over the Arctic was such that more thick multi-year ice north of Greenland was exported through Fram Strait (Walsh and Chapman 1990). According to these simulation results, the export of Beaufort Sea ice anomalies out of the Arctic contributes a small (7% compared to at least 25%) but still notable amount to the fluctuations in fresh water input to the Greenland Sea.

5 Conclusions

The possible causes of interannual variability of the sea-ice cover in the Beaufort-Chukchi Sea are investigated. The three factors considered include the effects of upper ocean stratification (due to Mackenzie river runoff), atmospheric temperature and wind stress anomalies. Based on simple first-order calculations, analysis of atmospheric temperature and wind stress data, and sea-ice model simulations, we conclude that anomalous wind patterns in the western Arctic are the principal cause of sea-ice interannual variability in the Beaufort-Chukchi Sea. In particular, a simulation of the 1964–65 sea-ice cover forced with 1964–65 wind stresses and climatological atmospheric temperature could reproduce very well the observed anomalous ice conditions. In contrast, when forced with the climatological wind stress and 1964–65 atmospheric

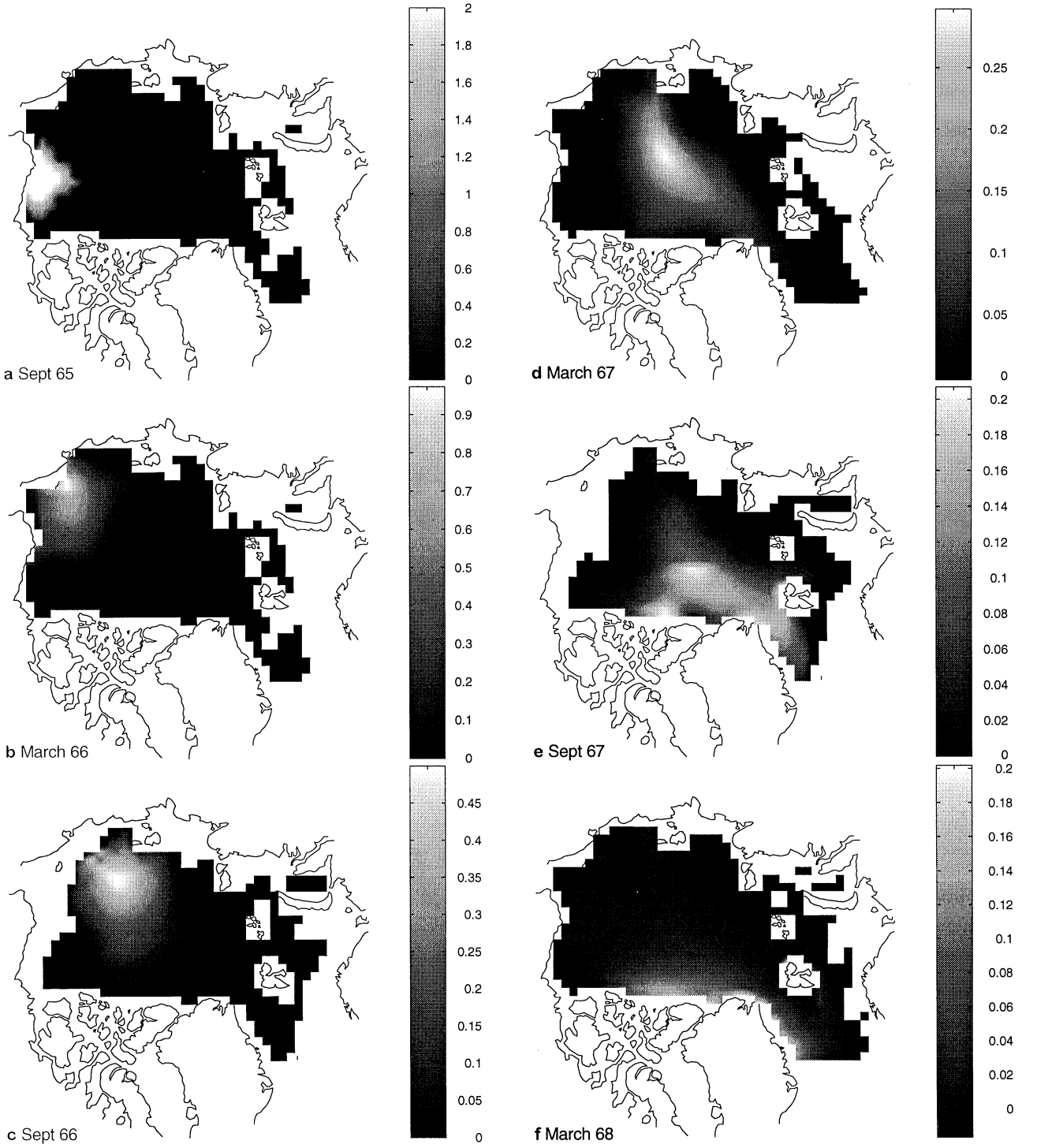

Fig. 3a–f Difference in sea-ice thickness fields starting in October 1965. The time interval between two figures is six months. *Thickness scales* to the *right* of each figure are in *meters*; *note* that each *colorbar* has a different *scale*

temperatures, the Beaufort sea-ice conditions are very similar to climatology. The influence of anomalous atmospheric temperature on anomalous ice conditions is believed to play an important role for longer time scale fluctuations (2–3 y). Regarding the influence of sea surface salinity on ice conditions, an analysis shows that a reduction in river runoff causing a decrease in stratification will have a larger influence on sea-ice conditions than an increase in river runoff. However, the fluctuations in the input of fresh water into the Arctic do not appear to be important in creating interannual variations in the sea-ice cover.

The possibility that ice anomalies in the western Beaufort Sea could be advected around the Beaufort Gyre and into the Transpolar Drift Stream and thus lead to a notable anomaly in the sea-ice export out of the Arctic through Fram Strait is also studied. A three-year simulation showing the time evolution of an ice anomaly representative of the one observed in the western Beaufort Sea in 1965, was also performed. The results show that after 2.0 y, the ice anomaly had reached the Fram Strait and still had 10% of its original magnitude. For a typical spring ice thickness in the Fram Strait of 3 m, this constitutes a 7% ice volume anomaly, which is small compared with the ice concentration anomaly of 25% (Mysak and Power 1992) observed in this region from satellite data. We conclude that ice conditions in the peripheral seas in the Arctic basin can contribute to small but detectable variations in ice export from the Arctic into the Greenland Sea.

Acknowledgements We are grateful to Prof. R. G. Ingram for carefully reviewing Sect. 3.1 and Appendix A of this manuscript and to the reviewers for their helpful comments. L.-B.T. thanks NSERC and Fonds FCAR for scholarship support during the course of this work, and L.A.M. is indebted to AES and NSERC for research grant support. Finally, we thank Prof. John Walsh from the University of Illinois for having provided the sea ice concentration data and Dr E.C. Carmack for the T-S data.

Appendix A

The influence of river runoff on ocean surface salinity and mixed-layer depth

In this section, we provide a more complete analysis of the effect of river runoff on the sea surface salinity and mixed-layer depth. In spring, fresh water from river runoff and sea ice melt mixes with deeper saltier ocean water under the action of waves, winds and tides, resulting in a rise in the potential energy of the system. Keeping the energy input (or rise in potential energy) constant from year to year, the influence of variable river runoff on the mixed-layer depth and sea surface salinity can be isolated.

Figure 4 shows the ocean surface layer before and after mixing of fresh water from river runoff and sea ice melt has occurred. The rise in the potential energy of the system per unit area after mixing, can be written as follows (see Gill 1982, p 139):

$$\rho_1 H_{ml} g \frac{H_{ml}}{2} - \left[\rho_2 (H_{ml} - h_f) g \frac{H_{ml} - h_f}{2} + \rho_w h_f g (H_{ml} - h_f/2) \right]$$

where ρ_1 is the average density of the water below the mixed layer, ρ_1 and ρ_w are the mixed-layer and fresh water densities, g the gravitational acceleration, H_{ml} the mixed-layer depth, h_f the thickness of the fresh water layer, equal to $(Q_M + Q_{im})/A_{BS}$, where Q_M and Q_{im} are the average volume input of fresh water from the Mackenzie River and sea ice melt, and A_{BS} is the Beaufort Sea surface area. In the equation, the reference level for the calculation of the potential energies is taken at the base of the mixed layer (Fig. 4b). From the conservation of mass principle, the density of the mixed layer, ρ_1, can be written in terms of the fresh water layer thickness h_f and other constants (ρ_2, ρ_w and H_{ml}) as follows:

$$\rho_1 = \rho_2 - (\rho_2 - \rho_w) \frac{h_f}{H_{ml}}.$$

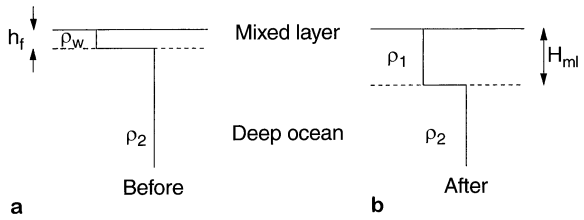

Fig. 4a, b Schematic of the ocean surface layer **a** before, and **b** after, mixing with the deeper ocean took place

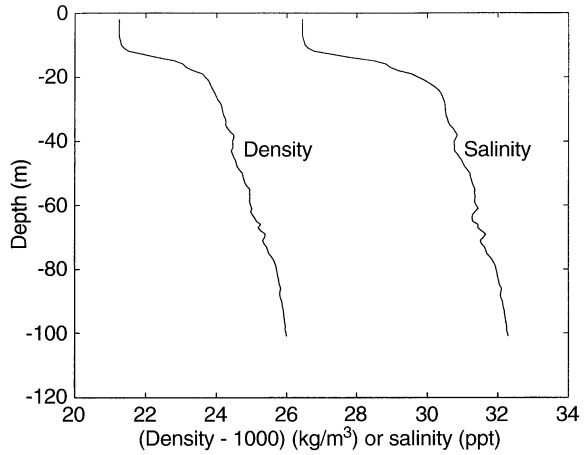

Fig. 5 Density and salinity depth profiles in the western Beaufort Sea. Data provided by E.C. Carmack

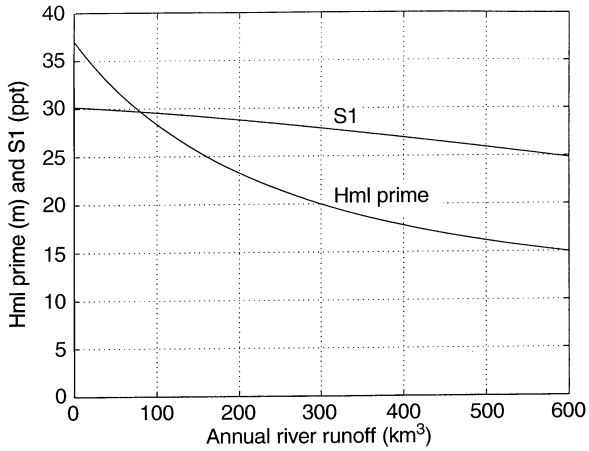

Fig. 6 Mixed-layer depth and salinity as a function of Mackenzie River annual runoff

Thus the rise in potential energy of the system per unit area can be written as

$$\frac{1}{2}(\rho_2 - \rho_w) g h_f (H_{ml} - h_f).$$

The salinity of the surface layer after mixing has occurred can be written as follows:

$$S_1 = \frac{H_{ml} - h_f}{H_{ml}} S_2, \tag{3}$$

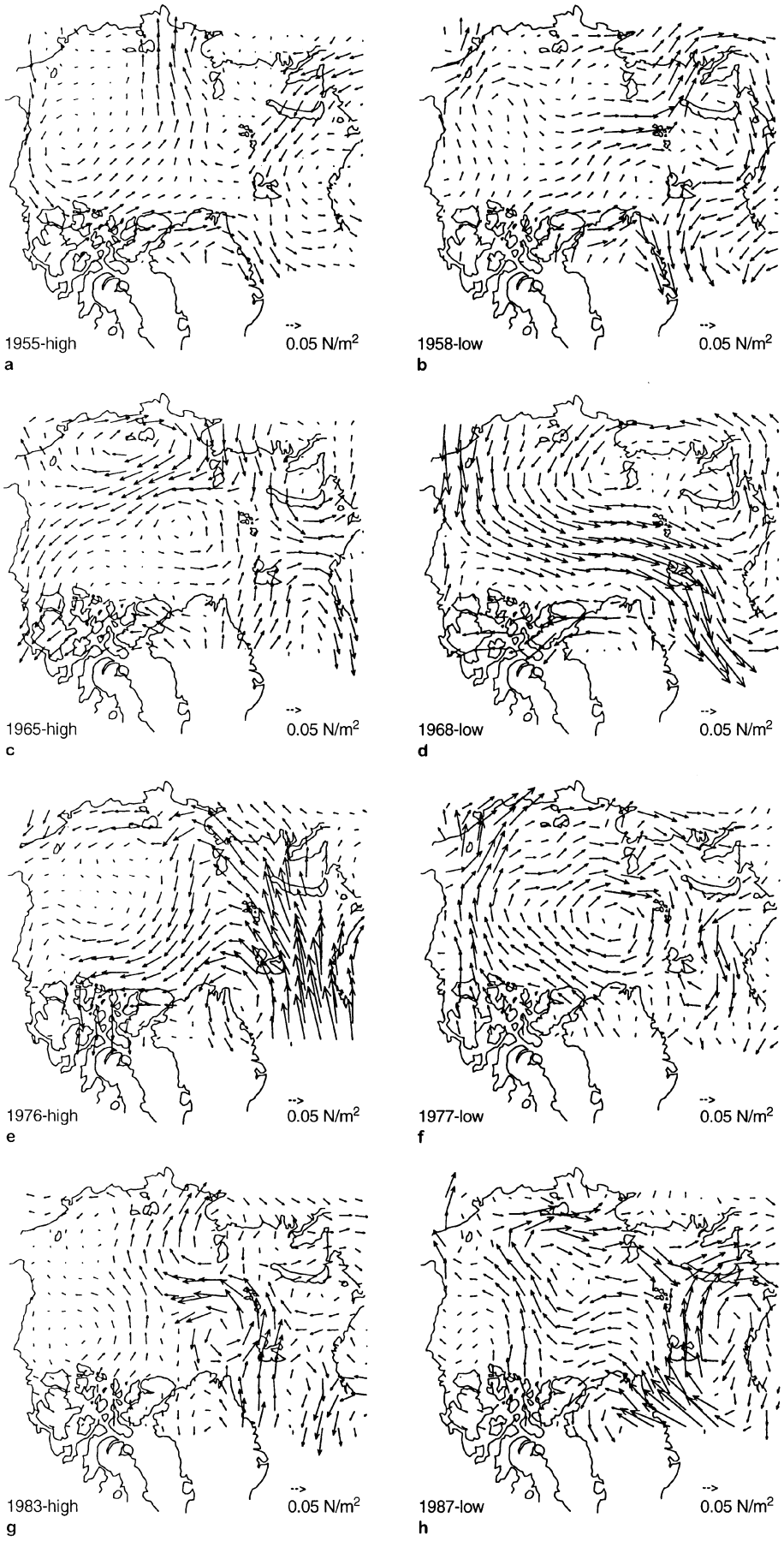

Fig. 7a–h Wind stress anomalies (spring-summer) for the years **a** 1955 **b** 1958, **c** 1965, **d** 1968, **e** 1976, **f** 1977, **g** 1983 and **h** 1987. These are computed as departures from the climatological wind stresses calculated from these 8 y

where S_1 is the mixed layer salinity and S_2 is an average salinity below the mixed layer. For a mixed layer depth of 20 m (Fig. 5), S_2 of 31 ppt, a Mackenzie River runoff of 300 km^3 spread uniformly over the Beaufort Sea area (300×10^3 km^2) and a sea-ice melt thickness of 1 m, the thickness of the fresh water layer (h_f) is 2 m and the salinity difference between the top and bottom layer calculated from Eq. 3 is 3.1 ppt. This is in general agreement with measurements made in the western Beaufort Sea (see Fig. 5).

Assuming the rise in the potential energy of the system remains the same from year to year, we have

$$h'_f(H'_{ml} - h'_f) = h_f(H_{ml} - h_f),$$

where H'_{ml} is the new mixed layer depth and h'_f the increase river runoff. Thus the new mixed layer depth (H'_{ml}) for an increase river runoff (h'_f) is

$$H'_{ml} = \frac{h_f}{h'_f}(H_{ml} - h_f) + h'_f. \quad (4)$$

Figure 6 shows the variation of the mixed-layer depth and salinity for a Mackenzie River runoff varying between 0 and twice the climatological value, as calculated from Eqs. 4 and 3. Figure 6 shows that increasing the river runoff has a smaller influence on the stratification than a reduction in river runoff. Also, for a 17% increase in Mackenzie River runoff, as observed in 1965, the reduction in mixed layer depth is approximately 1.2 m (Fig. 6); this results in a 0.48 ppt reduction in sea surface salinity (Fig. 6).

Appendix B

Monthly mean wind stresses for other anomalous years

The wind stress anomaly fields for eight years when abnormally high or low ice concentrations were present in the Beaufort-Chukchi Sea (1956–high, 1958-low, 1965-high, 1968-low, 1976-high, 1977-low, 1983-high and 1987-low), are shown in Fig. 7a–h. The wind stress fields are constructed from the spring (April–June) and summer (July–September) months; the fall and winter values are not considered since we focus on summer ice anomalies and the time scale associated with sea-ice advection is about two months (see Sect. 3). In previous data studies (Mysak and Power 1992), the influence of winds on ice conditions was assessed using the seasonal mean sea level pressure anomally fields (In this case, the wind stress is $\alpha|\vec{u}_a^2|$, where $\vec{u}_a$ is computed from the seasonal mean SLP) rather than the seasonal mean wind stress anomaly fields ($\alpha|\overline{\vec{u}_a^2}|$). These two fields can be significantly different, especially in the summer, when large wind events are usually associated with the passage of cyclones.

The results indicate (Fig. 7a–h) that years with positive ice anomalies are generally associated with anomalous northerly or westerly wind stresses which tend to push ice into the coastal region of the Beaufort-Chukchi Sea, while years with negative ice anomalies are generally associated with anomalous southerlies or easterlies which drive ice away from the coastal region of the Beaufort Sea (note that the ice drift direction is to the right of the wind stress vector). The year 1987 stands as an exception, but the anomalous ice conditions that year were not as severe (see Fig. 1). Also, an examination of the anomalous air temperature fields (not shown here) show no distinct pattern between air temperature and anomalous ice conditions. These results support the conclusions from the detailed 1965 sea-ice simulations.

These conclusions are also in accord with the results of Rogers (1977) who showed that ice concentration was highly correlated with local winds and weakly correlated with temperature. On longer time scales (two-to-three years), however, it has been shown that the atmospheric temperature and ice anomalies are significantly correlated (Manak and Mysak 1989; Rogers 1977).

References

Aagaard K, Carmack EC (1989) The role of sea ice and other fresh water in the Arctic circulation. J Geophys Res 94 : 14485–14498

Aagaard K, Swift JH, Carmack EC (1985) Thermohaline circulation in the arctic mediterranean seas. J Geophys Res 90 : 4833–4846

Bjornsson H, Mysak LA, Brown RD (1995) On the interannual variability of precipitation and runoff in the Mackenzie drainage basin. Clim Dyn 12 : 67–76

Bourke RH, Garrett RP (1987) Sea ice thickness distribution in the Arctic Ocean. Cold Regions Sci Technol 13 : 259–280

Broecker WS, Peteet DM, Rind D (1985) Does the ocean-atmosphere system have more than one stable mode of operation? Nature 315 : 21–26

Chapman WL, Welch WJ, Bowman KP, Sacks J, Walsh JE (1994) Arctic sea ice variability: Model sensitivity and a multidecadal simulation. J Geophys Res 99 : 919–935

Chouinard LE, Garrigues L (1995) Interannual variability of the ice cover in the Chukchi and Beaufort seas. In: Proc Fifth (1995) International Offshore and Polar Engineering Conference, The Hague, The Netherlands, pp 357–363. The International Society of Offshore and Polar Engineering

Dickson RR, Lamb HH, Malmberg S-A, Colebrook JM (1975) Climatic reversal in northerm North Atlantic. Nature 256 : 479–482

Gill AE (1982) Atmosphere-ocean dynamics. Academic Press

Goose H, Campin JM, Fichefet T, Deleersnijder E (1997) Sensitivity of a global ice-ocean model to the Bering Srait throughflow. Clim Dyn 13 : 349–358

Häkkinen S (1993) An Arctic source for the great salinity anomaly: a simulation of the Arctic ice-ocean system for 1955–1975. J Geophys Res 98(C9) : 16 397–16 410

Levitus S (1994) World ocean atlas 1994, CD-ROM data sets

Manak DK, Mysak LA (1989) On the relationship between Arctic sea-ice anomalies and fluctuations in northern canadian air temperature and river discharge. Atmos Ocean 27(4) : 682–691

Maykut GA, Untersteiner N (1971) Some results from a time-dependent thermodynamic model of sea ice. J Geophys Res 76 : 1550–1575

McPhee MG (1975) Ice-ocean momentum transfer for the aidjex ice model. AIDJEX Bull 29 : 93–111

Mysak LA, Manak DK (1989) Arctic sea-ice extent and anomalies, 1953–1984. AO 27 : 376405

Mysak LA, Manak DK, Marsden RF (1990) Sea-ice anomalies observed in the Greenland and Laborador seas during 1901–1984 and their relations to an interdecadal Arctic climate cycle. Clim Dyn 5 : 111–113

Mysak LA, Power SB (1992) Sea-ice anomalies in the western Arctic and Greenland-Iceland sea and their relation to an interdecadal climate cycle. Climatol Bull 26(3) : 147–176

Rogers JC (1977) A meteorological basis for long-range forecasting of summer and early autumn sea ice conditions in the Beaufort sea. In: Muggeridge DB (ed) Proc Fourth Int Conf on Port and Ocean Engineering under Arctic Conditions, pp 952–962, Memorial University, St-John's, Newfoundland

Tremblay L-B, Mysak LA (1997) Modelling sea ice as a granular material, including the dilatancy effect. J Phys Oceanogr 27 : 2342–2360

Walsh JE, Chapman WL (1990) Arctic contribution to upper-ocean variability in the North Atlantic. J Clim 3 : 1462–1473

Weatherly JW, Walsh JE (1996) The effects of precipitation and river runoff in a coupled ice-ocean model of the Arctic. Clim Dyn 12 : 785–798